ACADEMIC PRESS

Available online at www.sciencedirect.com

SCIENCE DIRECT®

Journal of Magnetic Resonance 164 (2003) 310–320

JMR Journal of Magnetic Resonance

www.elsevier.com/locate/jmr

Self-diffusion measurements by a constant-relaxation method in strongly inhomogeneous magnetic fields

M. Klein, R. Fechete, D.E. Demco, and B. Blümich*

Institut für Technische Chemie und Makromolekulare Chemie, Rheinisch-Westfälische Technische Hochschule, Worringerweg 1, Aachen D-52056, Germany

Received 21 March 2003; revised 11 June 2003

Abstract

The simple pulse sequence $\theta_x - \tau_1 - 2\theta_y - \tau_1 + \tau_2 - 2\theta_y - \tau_2 - Hahn\ echo$ used to measure the self-diffusion coefficient D under constant-relaxation condition, i.e., for $\tau_1 + \tau_2 = \text{const.}$ was investigated in the presence of strongly inhomogeneous static as well as radiofrequency magnetic fields. The encoding of the Hahn-echo amplitude by the pulse flip angle and diffusion was evaluated by taking into account the spatial distribution of the off-resonance field, the strength and orientation of the local field gradients, and the pulse flip angles by a computer simulation program. As input files, this program uses maps of static and radiofrequency fields, and the D coefficient can be evaluated from the time dependence of the Hahn-echo amplitude. The method was applied to a mobile one-sided *NMR* sensor, NMR-MOUSE with a bar magnet by measuring D for a series of liquids with different viscosities. The method was shown to be particularly useful for measuring D of solvents in elastomers without the need for measurements of the transverse relaxation rates. The self-diffusion coefficient of toluene in a series of crosslinked natural rubber samples was measured and correlated with the crosslink density. Finally, the method was applied to measure the diffusion anisotropy of free water in bovine Achilles tendon.
© 2003 Elsevier Inc. All rights reserved.

Keywords: NMR; ^{1}H self-diffusion; Strongly inhomogeneous magnetic fields; Unilateral NMR; NMR-MOUSE; Crosslinked elastomers; Diffusion anisotropy in tendon

1. Introduction

In the last few years, several NMR applications have been developed that operate in strongly inhomogeneous static and radiofrequency (rf) magnetic fields. They address topics like stray field NMR [1], the development of surface NMR spectrometers [2,3] with applications in material testing [4–7], biomedicine [8], and well logging [9–12]. Moreover, approaches toward high-resolution ex situ NMR spectroscopy have been discussed recently [13–15].

Investigations of molecular self-diffusion provide important information on molecular organization and interactions with the environment in many systems. The effect of molecular self-diffusion on the amplitude of the stimulated spin echo in a stationary strong magnetic-field gradient was analyzed theoretically and experimentally in recent years [10–12,16–20]. The method of strong static gradients has some advantages. One is the large gradient of the stray field of superconducting magnets, which allows measurements of root-mean square molecular displacements as small as 20 nm and self-diffusion coefficients as small as 10^{-16} m^2/s. The large gradients permit measurements of the diffusion coefficient in a simple way in heterogeneous materials like porous materials and biological systems, since it reduces the relative contribution from the background gradients. This is so because the background gradients are generally proportional to the magnitude of the applied static field B_0 but essentially independent of the field gradient. From this point of view measurements with unilateral low field NMR sensors which produce relatively strong field gradients is of advantage.

One particular aspect of diffusion measurements, is the influence of various relaxation processes on the

* Corresponding author. Fax: +49-241-8888-185.
E-mail address: bluemich@mc.rwth-aachen.de (B. Blümich).

1090-7807/$ - see front matter © 2003 Elsevier Inc. All rights reserved.
doi:10.1016/S1090-7807(03)00237-4

acquired data. This problem is more severe with the static-fringe-field method than with the pulsed-gradient stimulated-echo (PGSE) methods [21,22] (and references therein). In the case of gradient-strength encoding, if the dependence of relaxation times on the gradient strength can be neglected, the diffusion coefficient can be measured without knowledge of these competing nuclear magnetization transport parameters. For a static-stray-field gradient, only the time-encoding method can be applied. In this case, the transverse relaxation T_2 in the case of Hahn-spin echo, and for a stimulated echo the longitudinal relaxation time T_1 together with T_2 affect the signal in addition to diffusion. The effect of relaxation which complicate the self-diffusion diffusion measurements in a static-strong-field gradient can be overcome by constant-relaxation methods [17,19,23].

Woessner [24] has studied the effect of diffusion in inhomogeneous fields up to four pulses and Demco et al. [19] generalized this results taking into account the strong off-resonance effects during the radiofrequency pulses. The evolution of polarizations and coherences following any series of radiofrequency pulses in strongly inhomogeneous magnetic fields, with particular attention to diffusion and relaxation effects was analyzed by Hürlimann [12]. His theoretical approach follows Kaiser et al. [25] and decomposes the signal into the contributions from different coherent pathways. The diffusion effects were analyzed in the case of the Carr–Purcell–Meiboom–Gill pulse sequence and it was shown that unrestricted diffusion leads to non-exponential signal decay versus the echo number.

One of the goals of this paper is to implement a constant-relaxation method for measuring the self-diffusion coefficient (D) in strongly inhomogeneous magnetic fields. This method was implemented in the stray-magnetic field of a new bar-magnet NMR-MOUSE. The spatial distribution of the static and radiofrequency fields, as well as the static-magnetic-field gradients in the voxels of the sensitive volume were characterized by magnetic-field simulations and measurements. For the case of an isolated spin system, the total echo signal given by the sum of the signals from each voxel of the sensitive volume from different coherences, and z-polarizations encoded by diffusion was evaluated numerically. The effects of local off-resonance and rf pulse flip angle were taken into account in the C++ program used for simulation of the echo amplitude. The method was tested for different liquids with a broad distribution of diffusivities.

Another goal of this work is to show that the constant-relaxation method is advantageous in measuring ^{1}H self-diffusion coefficients of mobile molecules in complex protonated systems with strong restrictions in their molecular mobility. Two particular examples are discussed: (i) solvents in crosslinked elastomers and (ii) the anisotropy of the self-diffusion diffusion coefficient of free water in Achilles tendon.

2. Simulation of the diffusion encoded spin system response

In the following, the spin system response of a collection of isolated spins to the rf pulse sequence $\theta_x - \tau_1 - 2\theta_y - \tau_1 + \tau_2 - 2\theta_y - \tau_2 - \textit{Hahn echo}$ (cf. Fig. 1) is considered in strongly inhomogeneous static and rf magnetic fields. The pulse flip angle in the local rotating reference frame can be considered to have a well-defined value for each voxel of the sample. In general, in the sensitive volume the pulse flip angle θ is different from 90° and therefore, the pulse sequence will generate primary and secondary Hahn echoes as well as a stimulated echo [21,22]. The amplitude of the first secondary echo represents the NMR signal which is used for extracting the information on the self-diffusion coefficient D. If the constant time relaxation strategy is implemented [23], i.e., $\tau_1 + \tau_2 = \text{const.}$, when τ_1 and τ_2 are varied, the first secondary Hahn echo will be superimposed on the stimulated echo at $\tau_1 = \tau_2$ (see below).

For this simple pulse sequence, there are two procedures which can, at least in principle, be applied in order to evaluate the response of the spin system. The analytical method can use the evolution of the single-quantum coherences and polarization in the 3×3-dimensional Liouville space that can be described by the spin density operator formalism [19] (and references therein) or by simple rotations of the magnetization vector [12,25]. The rotations of the magnetization components takes place around an effective field specific to each voxel and defined by the local off-resonance fields and the strength of the component of the rf field normal to the static magnetic field $\vec{B}_0(\vec{r})$.

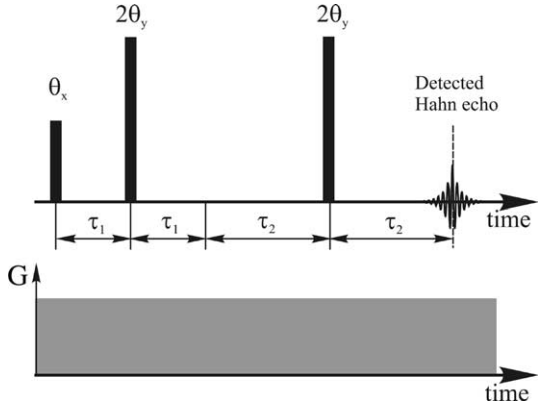

Fig. 1. Hahn-echo pulse sequence for time constant relaxation for measurements of diffusion coefficient. The flip angles θ and 2θ of the radiofrequency pulses correspond to a voxel in the sample, and $\tau_1 + \tau_2 = \text{const.}$

A computer program was written in C++ to generate analytical expressions for all the coherences and the z-polarization which contribute to the Hahn echo detected at time $2(\tau_1+\tau_2)$. Unfortunately, we have received about 10^3 coherences and polarizations which describe the behavior of the Hahn echo. Hence, we found that a procedure based on the analytical solution to evaluate the NMR signal is extremely difficult to implement.

Because the pulse sequence discussed before is working in the strongly inhomogeneous magnetic fields characteristic for unilateral NMR the signal has to be evaluated by numerical simulation. It was shown before [4] that such NMR signal simulation comprises four steps: (i) computation of the static magnetic field $\vec{B}(\vec{r})$ and the field gradient in each of the volume elements; (ii) computation of the normal rf field components at the same points; (iii) calculation of the evolution of the local magnetization vector under the influence of the pulse sequence; and (iv) calculation of the electric signal induced in the surface coil by the nuclear spins.

The C++ program written follows the steps discussed above. The rotation of the magnetization components and the free evolution periods are evaluated numerically for each voxel with τ_1 and τ_2 as parameters with the condition $\tau_1+\tau_2=\text{const}$. The simulation is repeated for each voxel of the sensitive volume and the results are added to obtain the overall NMR signal. The diffusion encoding was introduced on the lines discussed in [19,21,22]. The normalized Hahn-echo amplitude from the voxel specified by the vector $\vec{r}$ is encoded by the diffusion process according to [19,23]

$$\frac{E(\tau_1;\tau_2;\vec{r})}{E(\tau_{10};\tau_{20};\vec{r})}\propto\exp\left\{-\frac{2}{3}\gamma^2G^2(\vec{r})D\left(\tau_1^3+\tau_2^3\right)\right\}, \tag{1}$$

where γ is the magnetogyric ratio and $(\tau_{10};\tau_{20})$ is the initial pair of time parameters for the constant time relaxation pulse sequence (cf. Fig. 1). In Eq. (1) it is assumed that the gradient on the length scale of diffusive displacement is constant (see below). By normalization, any dependence on the local transverse magnetization relaxation is eliminated in the first approximation. In reality, this is strictly valid only for each individual voxel. If the heterogeneity of the transverse relaxation can be neglected, the normalization procedure applied to the sum of the signals from all the voxels in the sensitive volume leads to a quantity independent of T_2.

While varying τ_1 and τ_2 with $\tau_1+\tau_2=\text{const.}$, a particular situation is reached when $\tau_1=\tau_2=\tau$. Then the first secondary Hahn echo and the stimulated echo are superimposed. The encoding of the amplitude of these echoes by the pulse flip angle, relaxation, and diffusion is given by

$$E(\tau_1;\tau_2;\vec{r})\propto\sin^5(\theta)\exp\left\{-\frac{4\tau}{T_2}\right\}\exp\left\{-\frac{4}{3}\gamma^2G^2(\vec{r})D\tau^3\right\} \tag{2}$$

for the Hahn echo, and by

$$E(\tau_1;\tau_2;\vec{r})\propto\frac{1}{2}\sin(\theta)\sin^2(2\theta)\exp\left\{-\frac{2\tau}{T_2}\right\}\times\exp\left\{-\frac{8}{3}\gamma^2G^2\left(\vec{r}\right)D\tau^3\right\} \tag{3}$$

for the stimulated echo. The pulse flip angle encoding in Eqs. (2) and (3) can be easily derived using the formalism presented in [19]. If a normalization of the sum of these two echo amplitudes is made using the initial amplitude of the Hahn echo a constant encoding with T_2 remains for the stimulated echo. Moreover, from the above equations, it is evident that the encoding by diffusion is different for the two echoes. In order to avoid this complication the data corresponding to $\tau_1=\tau_2=\tau$ were removed. The effect discussed above is related to the presence of the stimulated echo that is generated only for the pulse sequences with flip angles $\theta\neq 90°$, i.e., in strongly inhomogeneous static magnetic fields.

For the simulation program the voxel size was chosen to be $2\,\mu\text{m}\times 2\,\mu\text{m}$ in the rz-plane resulting in a number of 415,426 voxels in the sensitive volume of the barmagnet NMR-MOUSE. The experimental data were analyzed by a least square fitting procedure. A simulation of a diffusion curve takes several hours on a 1.7 GHz Pentium 4 PC with 1024 Mbytes SDRAM memory.

3. Experimental

3.1. Samples

Low viscosity liquids 1,2-propandiol and glycerin were purchased from Fluka Chemie AG, and from Sigma–Aldrich, respectively. High viscosity liquids polyethyleneglycol with a molar mass $M_w=10{,}000$ g/mol and silicon oil SLM 55006 with $M_w=5200$, were acquired from Aldrich Chemie and Wacher-Chemie GmbH, Germany.

In addition of these liquids a series of different crosslinked samples from commercially available natural rubber (NR) SMR10 (Malaysia) was investigated. The additives were 3 phr (parts-per-hundred-rubber) ZnO and 2 phr stearic acid. The sulfur and accelerator contents of the samples are given in Table 1. The accelerator is of the standard sulfenamide type (TBBS, benzothiazyl-2-*tert*-butyl-sulfenamide). After mixing the compounds in a laboratory mixer at 50 °C, the samples were vulcanized at 160 °C in a Monsanto MDR-2000-E

Table 1
Properties of the series of crosslinked NR samples

Sample	Sulfur-accelerator content (phr)	Shear modulus[a]	Equilibrium toluene concentration[b]
		G (dNm)	c_s (%)
NR1	1–1	5.2	0.652
NR2	2–2	8.5	0.671
NR3	3–3	11.2	0.678
NR4	4–4	13.2	0.692
NR5	5–5	14.5	0.712
NR6	6–6	15.4	0.750
NR7	7–7	16.2	0.800

[a] The uncertainties are less than 10%.
[b] The uncertainties are less than 1%.

vulcameter. The degree of crosslinking was measured by the low frequency shear modulus or torque at a temperature of 160 °C in the vulcameter directly after vulcanization. The measurements were performed with an oscillation amplitude of ±0.5° and a frequency of 1.67 Hz. The natural rubber sampler were swollen in toluene for several hours until the equilibrium value was reached.

Samples of sheep Achilles tendon were obtained from the butcher. The samples were kept at −18 °C after excision until the time of measurements which were performed at room temperature 20 ± 1 °C. A plug was cut from the middle of the tendon and was wrapped with teflon tape in order to avoid dehydration. NMR measurements for each set of the orientation angles were made on at least three different tendon plugs to account for biological heterogeneity.

3.2. NMR experiments

The concept of an unilateral NMR sensor with a bar permanent magnet was introduced in order to search for a more uniform space distribution of field gradients in the sensitive volume [26] compared with the u-shape magnet of the conventional NMR-MOUSE sensor [3]. The geometrical configuration of NMR sensor used in the present measurements is shown in Fig. 2. Details concerning the magnet and the rf spiral coil are given in [27]. The diffusion coefficients measurements were preformed on ^{1}H with the pulse sequence of Fig. 1 using a pulse of duration of 4.2 μs and a repetition delay of 1–10 s. Bar-magnet NMR-MOUSE was operated by a Bruker Minispec spectrometer at the carrier frequency of 19.7 MHz.

The self-diffusion coefficients of water, propandiol, polyethylenglycol, silicon oil, and toluene in NR samples were also measured by the pulsed gradient stimulated echo method (PGSE) [21,22] and the time constant relaxation pulse sequence of Fig. 1 with a Bruker DMX 300 NMR spectrometer operating at ^{1}H frequency of

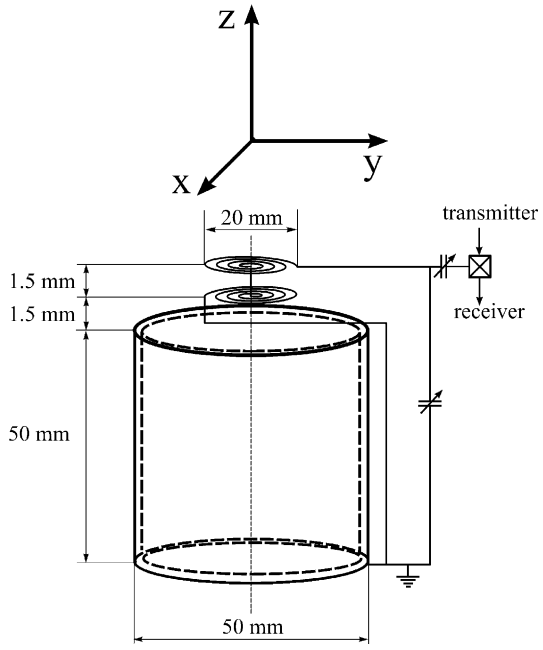

Fig. 2. Geometry of the bar magnet NMR-MOUSE. The permanent magnet with a cylindrical shape (dashed lines) is surrounded by a cooper shield. A double spiral coil is positioned on the top of the bar magnet.

299.87 MHz. In these measurements the 90° pulse length was 11 μs, and the strength of the constant magnetic-field gradient was $G_z = 0.142$ T/m. For PGSE method, the maximum strength and duration of the gradient pulses were 0.474 T/m and 1 ms, respectively. The gradient strength was changed in 64 equidistant steps.

4. Characterization of bar-magnet NMR-MOUSE

4.1. Field gradient map and sensitive volume

The evaluation of the self-diffusion coefficients using the simulation program discussed above needs the space distribution of the field gradients and the parameters of the sensitive volume. The field gradient map can be evaluated from the simulation of the static-magnetic-field map. These have been obtained using the finite element analysis program OPERA 3D from Vector Fields for a cylindrical shape permanent magnet made of NdFeB. The radial component B_{0r} (a) and the axial component B_{0z} (b) of the static magnetic field and the strength B_0 (c) are shown in Fig. 3. B_{0z} was also measured at the surface of the radiofrequency coil by a homemade scanning device equipped with a Hall probe. The measured map is shown in Fig. 4a, and the simulation of the B_{0z} map is shown in Fig. 4b. The differences between the two maps come about from the finite size of the Hall probe.

The map of the square of the static-magnetic-field gradient (G^2) can be obtained from the field components maps (see Figs. 3a and b) considering that for each voxel the changes in the magnetic field can be approximated by a linear magnetic field. The map of G^2 is shown in Fig. 5a. It is evident that the spatial distribution of the field gradient is, in general, non-uniform. The apparent discontinuities of the G^2 distribution shown in Fig. 5a are due to the numerical artifacts. Nevertheless, the static magnetic field along the z-direction that is shown in Fig. 5b is to a good approximation linear.

The sensitive volume can be simulated if also the map of the components of the radiofrequency field normal to $B_0(\boldsymbol{r})$ are known. Figs. 6a and b depict the radial (B_{1r}) and normal (B_{1n}) components of the radiofrequency field of a spiral cooper coil for a current of intensity $I = 1\,\mathrm{A}$ computed by the program OPERA 3D Vector Fields. The space distribution of the NMR signal, i.e., the sensitive volume can be evaluated using the procedure described in [4] (cf. Fig. 7). In the simulation of the sensitive volume two filters were applied: the first one accounts for the quality factor $Q = 20$ for the NMR coil and the other for the spectrometer bandwidth. If we compare the space distribution of the NMR signal with the G^2 map (cf. Fig. 5a) it is evident that the magnetic field gradient is not uniform across the sensitive volume. This fully justifies our effort to develop a numerical program which describes the overall NMR echo signal

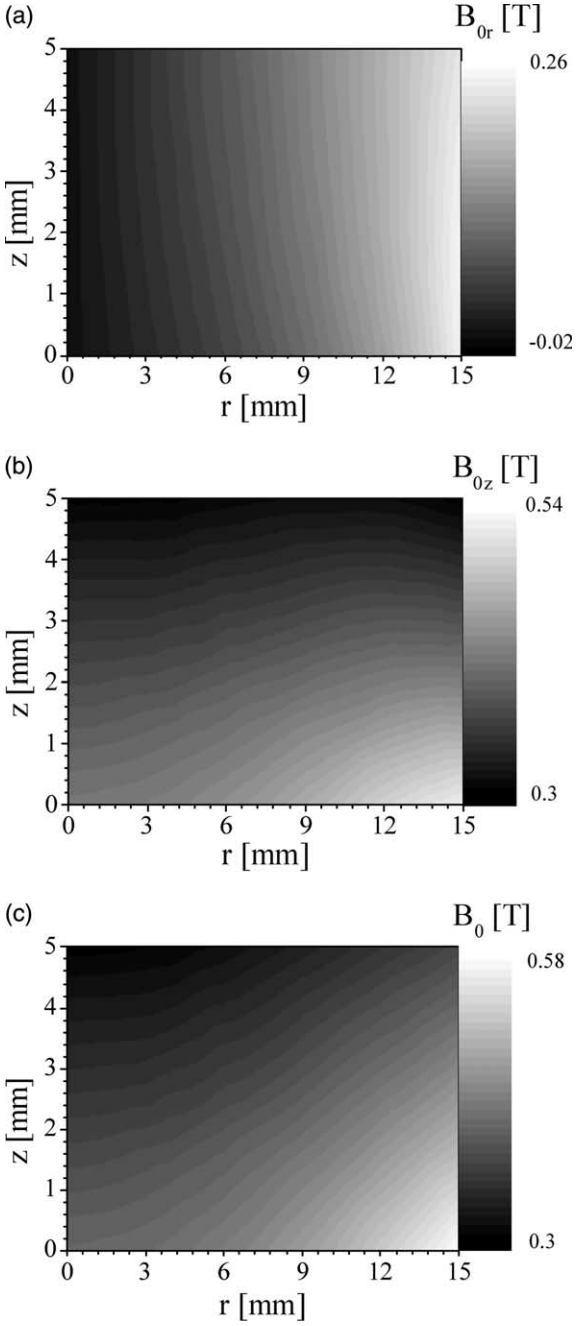

Fig. 3. Simulated static magnetic field maps. Maps of the local radial component B_{0r} (a), the component along the local static magnetic fields B_{0z} (b), and the magnitude of the local magnetic field B_0 (c) maps were simulated using finite element analysis program Opera 3D from Vector Fields.

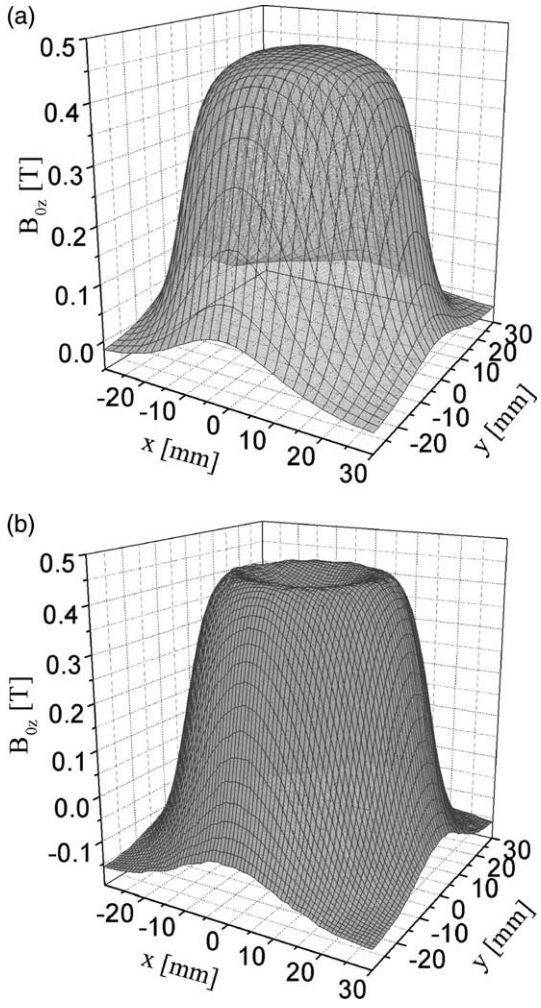

Fig. 4. Measured (a) and simulated (b) distributions of the static magnetic field for the cylindrical bar magnet at the magnet pole face ($z = 0$). The z-axis is parallel to the cylinder axis of the magnet.

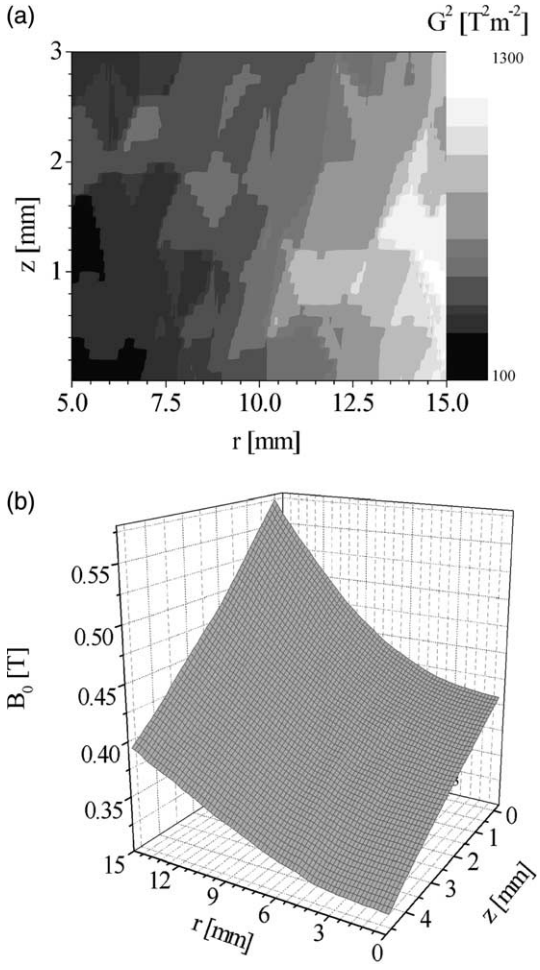

Fig. 5. (a) Space distribution of the square of the static magnetic field gradient G. (b) The variation of the strength of the static-magnetic field along the z-direction at different radial positions.

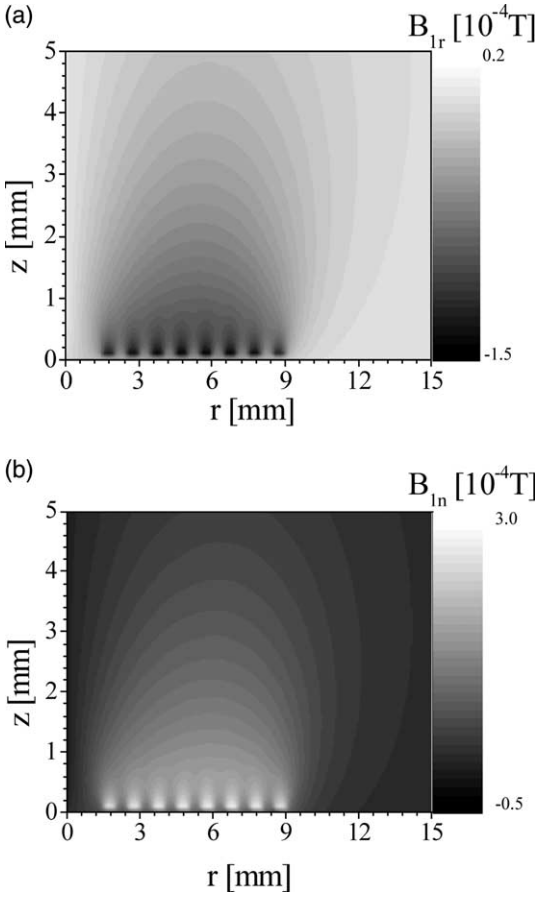

Fig. 6. (a) Simulation of the radial component of the radiofrequency magnetic field of a spiral coil with eight turns (cf. Fig. 1). (b) Simulation of the space distribution of the component of the amplitude of the radiofrequency field normal to the local direction of the static magnetic field $\vec{B}_0(\vec{r})$. The effective intensity of the current in the coil is $I_{\text{eff}} = 1\,\text{A}$. The origin of the coordination system was taken in the centre at the surface of the magnet.

as a sum of the signals originating from individual voxels.

4.2. Self-diffusion measurements

To test the performance of the bar-magnet NMR-MOUSE in measuring self-diffusion coefficients, the time constant relaxation method (see Fig. 1) was applied to distilled water at room temperature. The normalized values of the Hahn-echo amplitude are shown in Fig. 8a for the pulse sequence with $\tau_1 + \tau_2 = 0.5\,\text{ms}$. The numerical simulation was performed using the program described in chapter 2 (black circles in Fig. 8a). From the simulation and measurements the data taken at $\tau_1 \approx \tau_2$ were excluded where the simulated and Hahn echoes are superimposed (cf. Fig. 8a). The self-diffusion coefficients estimated from this simulation is $D = (2.25 \pm 0.05) \times 10^{-9}\,\text{m}^2\text{s}^{-1}$ in a good agreement with the reported value of $D = 2.023 \times 10^{-9}\,\text{m}^2\text{s}^{-1}$ measured at 20 °C (Bruker Almanac 2002). This also support the assumption of a linear gradient on the length scale of diffusive displacement (see Eq. (1)). Moreover, this also proves that the simulation program provides reliable results.

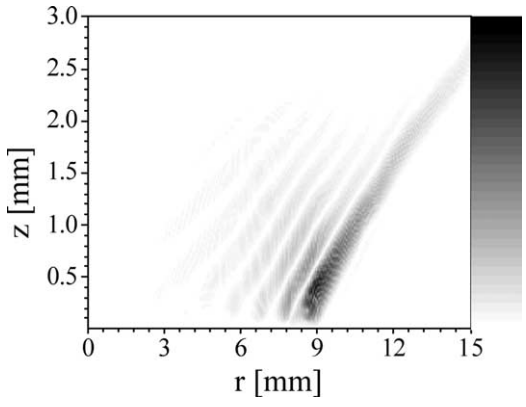

Fig. 7. Simulated space distribution of the sensitive volume of the bar magnet NMR-MOUSE with the geometrical configuration shown in Fig. 1. The echo signal generated by the pulse sequence of Fig. 1 was elaborated with the program described in Section 2.

As another test of the performances of the constant time relaxation method the diffusion coefficient of water was measured with a Bruker DMX-300 NMR spectrometer in the presence of a constant field gradient. The data are shown for a pulse flip angle of $\theta = 90°$ (cf. Fig. 1) in Fig. 8b. The changes in the echo amplitude at the values of τ_1 where the stimulated and Hahn echoes start to be superimposed are evident. The simulation program for a constant field gradient provides a diffusion curve (not shown in Fig. 8b) which is in a good agreement with the experimental data, giving an estimated value of the diffusion coefficient of $D = 2.27 \times 10^{-9}\,m^2s^{-1}$ (see above). It is clear from Figs. 8a and b that the overall shape of the diffusion encoded amplitude of the Hahn echo are the same for the case of a space constant linear magnetic gradient field and a complex space distribution of field gradients present in the case of NMR-MOUSE.

5. Results and discussion

5.1. Self-diffusion coefficients of liquids with different viscosities

The possibility to measure self-diffusion coefficients for liquids with a relatively broad range of diffusion coefficients was investigated by time constant relaxation method (cf. Fig. 1) with the NMR-MOUSE. The measured data points are shown in Fig. 9a (open symbols) for toluene ($\tau_1 + \tau_2 = 0.5$ ms), propandiol ($\tau_1 + \tau_2 = 1.6$ ms), and glycerin ($\tau_1 + \tau_2 = 3.1$ ms). The results of the numerical simulations performed with the program described in chapter 2 are shown by black circles in Fig. 9a. The best fit of the experimental data leads to the values of diffusion coefficients listed in Table 2. For these low viscosity liquids the values of self-diffusion coefficients reported in the literature or measured on the

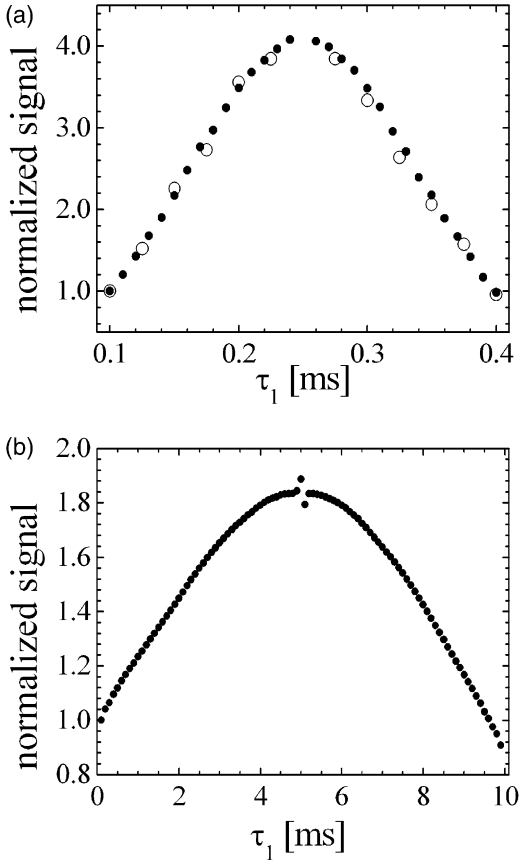

Fig. 8. (a) Normalized amplitudes of the Hahn echoes for the pulse sequence of Fig. 1 applied to distilled water at room temperature for $\tau_1 + \tau_2 = 0.5$ ms. Open circles: experimental data from bar- magnet NMR-MOUSE and black circles: simulated data. (b) Normalized Hahn-echo amplitudes acquired at 300 MHz with a Bruker NMR spectrometer for a pulse flip angle of 90° (b) for $\tau_1 + \tau_2 = 10.1$ ms. A time constant gradient $G_z = 0.142$ T/m was applied during the pulse sequence.

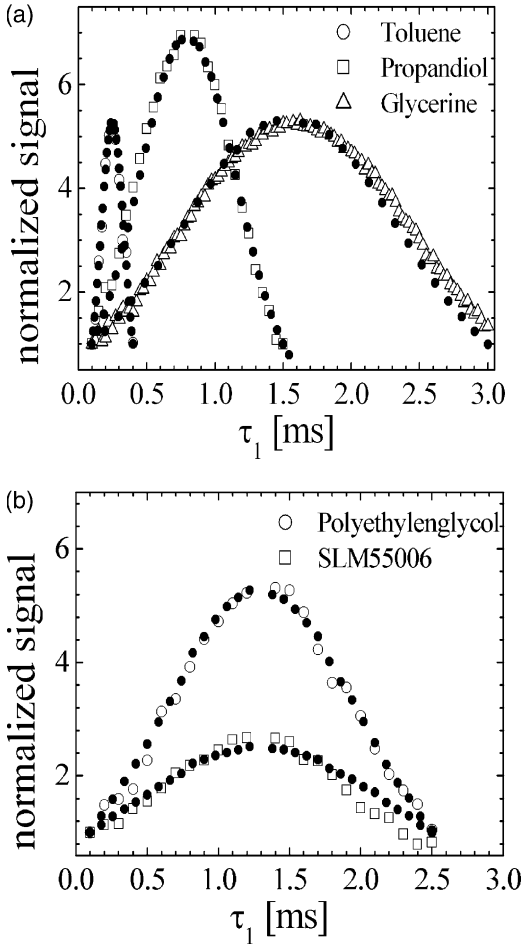

Fig. 9. Normalized Hahn-echo amplitudes measured with the pulse sequence of Fig. 1 versus τ_1 for $\tau_1 + \tau_2 = \text{const}$. Experimental data obtained with the NMR-MOUSE for toluene, propandiol and glycerol (a) and liquid polymers polyethylenglycol and silicon oil (SLM55006). Simulated data are shown by filled symbols. The resultant values of the diffusion coefficients are listed in Table 1.

Table 2
Self-diffusion coefficients D measured on liquids using the time constant relaxation method with a bar magnet NMR-MOUSE. In the last column the values of the diffusion coefficients from literature or measured are also given

Liquid	Self-diffusion coefficients by the NMR-MOUSE[a] D (10^{-9} m^2 s^{-1})	Self-diffusion coefficients from the literature or measured D (10^{-9} m^2 s^{-1})
Toluene	2.7	2.27[b]
Propandiol	0.045	0.041[d]
Glycerine	0.0047	0.00215[c]
Polyethylenglycol	0.0082	0.0087[d]
Silicon oil (SLM5506)	0.0045	0.0049[d]

[a] The uncertainties are less than 15%.
[b] Reported in the Bruker Almanac 2002
[c] S. Fernbach, W.G. Protcor, J. Appl. Phys. 26 (1955) 170–181.
[d] The D values were measured using PGSE on DMX-300 Bruker NMR spectrometer

same samples using PGSE method on DMX-300 NMR spectrometer are also given in Table 2. They differ by about 20% from the values measured with NMR-MOUSE. These differences are expected from the inaccuracy in the magnetic field maps from local magnet heterogeneities. Moreover, a change in the sample temperature during the measurements with NMR-MOUSE was detected which influences the diffusion measurements.

Polymer liquids with lower values of the self-diffusion coefficients were also measured. The large value of the average field gradient allows for an efficient diffusion encoding of the Hahn-echo amplitude. Normalized signals are shown in Fig. 9b for polyethylenglycol and silicon oil (SLM5506) comparing experimental data (open symbols) and the numerical simulation (black circles). The values of the diffusion coefficients are reported in Table 2. These values compare well with those obtained from measurements using PGSE method on DSM-300 NMR spectrometer (see Table 2).

5.2. Proton diffusion anisotropy of swelled toluene in crosslink series of natural rubber

The diffusion of light penetrant molecules in elastomers is a topic of long standing interest [28] (and references therein). It was shown that for small solvent molecules both transverse relaxation time and diffusion coefficient are sensitive measures of the free volume and its changes with filler content [29]. A free-volume theory of mass transport has been developed by Vrentas and Ventras [30] for predicting the solvent self-diffusion coefficients for rubbery polymer–solvent systems. For these systems, the solvent self-diffusion coefficient D, can be determined using the following equation:

$$D = D_0 \exp\left\{-\frac{E^*}{RT}\right\} \exp\left\{-\frac{c_s \hat{V}_s^* + (1-c_s)\hat{V}_p^*}{\hat{V}_{FH}/\gamma}\right\}, \quad (4)$$

where D_0 is a preeexponential factor, E^* is related to the energy per mole that a molecule needs to overcome attractive forces which hold it to its neighbors. $\hat{V}_i^*$ is the specific hole free volume of component $i = s$ (solvent) and $i = p$ (polymer) and c_s is the weight concentration of solvent in the system. The quantity $\hat{V}_{FH}$ is the average hole free volume per unit mass of the mixture, and γ represents an average overlap factor which is introduced because the same free volume is available to more than one jumping unit. One can write [30]

$$\frac{\hat{V}_{FH}}{\gamma} = c_s \frac{K_{ss}}{\gamma_s}\left(K_{ps} + T - T_{gs}\right) + (1-c_s)\frac{K_{sp}}{\gamma_p}\left(K_{pp} + T - T_{gp}\right), \quad (5)$$

where γ_i ($i = s, p$) represents the overlap factor for the free volume of pure component i. The quantities K_{ss} and K_{sp} are free-volume parameters for the solvent and K_{pp} and K_{ps} are free-volume parameters for the polymer. In Eq. (5) T is the temperature and T_{gi} is the glass transition temperature of the pure component i.

The functional form of the solvent concentration dependence of the diffusion coefficient D is rather complex (see Eq. (4)). The diffusion coefficient will increase monotonically with increasing c_s, and this curve is characterized by $\partial(\ln D)/\partial c_s > 0$ and $\partial^2(\ln D)/\partial^2 c_s < 0$ (negative curvature). This behavior is shown, for instance, by toluene imbedded in polystyrene [30] and also for our data (see below).

The diffusion coefficients of toluene swollen in the samples of a crosslink series of natural rubber (NR) (cf. Table 1) were measured by the constant time relaxation method and the NMR-MOUSE. The data shown by the open symbols in Fig. 10a are for NR1, NR4, and NR7. They were fitted with the program described in chapter 2 (black circles in Fig. 10a) and the diffusion coefficients were estimated. The dependences of the logarithm of diffusion coefficient versus the weight concentration at equilibrium c_s for a series of crosslinked NR (cf. Table 1) are shown in Fig. 10b. The functional dependence follows qualitatively the functional dependence given by Eq. (4). Moreover, the diffusion coefficients of toluene in samples NR1 and NR7 were measured for the same samples at 300 MHz by the pulsed gradient stimulated echo method [21,22] (Fig. 10b open symbols). These coefficients differ by about 20% from those measured with NMR-MOUSE. This is probably due to the heterogeneity of the permanent magnet that is not taken into account in the field simulation. At the same time the samples have a heterogeneous distribution of the transverse magnetization relaxation. Moreover, we shall

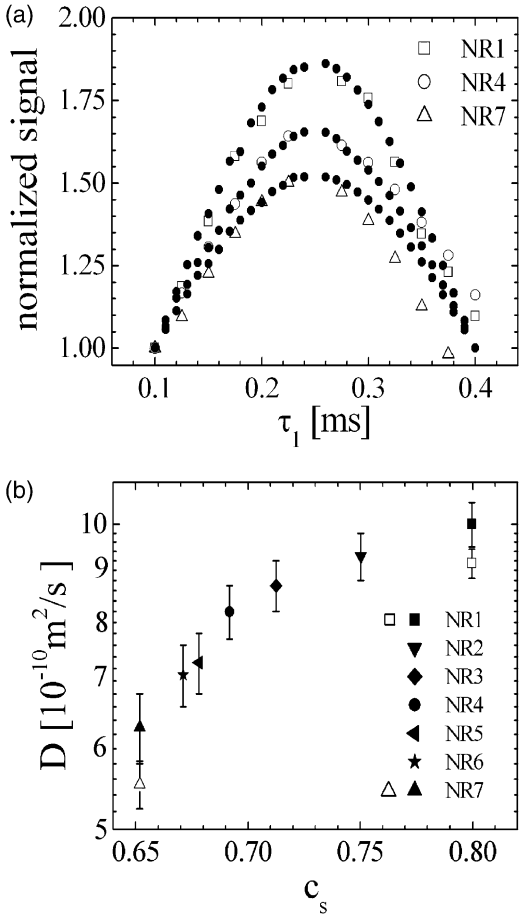

Fig. 10. Experimental data, fitted curves and self-diffusion coefficients of toluene in the samples from a crosslink series of natural rubber (see Table 2). (a) The normalized Hahn-echo amplitude (open symbols) measured with time-constant relaxation method for $\tau_1 + \tau_2 = 0.5$ ms for samples NR1, NR4, and NR7. The fit with the simulated values (black circles) produces the diffusion coefficients. They are shown in (b) versus the mass concentration (c_s) of the imbibed toluene. The measurements of the diffusion coefficients for NR1 and NR7 obtained by the same method with a high-field 300 MHz NMR spectrometer are also shown (open symbols).

note that there is a contribution to the Hahn echo from the elastomer protons that is not encoded by diffusion but just only by transverse relaxation. This contribution can be neglected in the first approximation because of the high equilibrium concentration of toluene and the much shorter value of T_2^* for the polymer chains.

5.3. Proton self-diffusion anisotropy of free water in bovine Achilles tendon

Tissues that have a regularly ordered microstructure, such as white brain matter and cardiac and skeletal muscle, reveal a marked anisotropy in the diffusion properties [31]. The proton self-diffusion anisotropy of bovine Achilles tendon was measured using a pulsed gradient spin echo with a superconducting magnet operating at 1.5 T [32]. The anisotropy is due to the existence of free water confined in the nanoscopic regions between the collagen fibrils well oriented along the macroscopic axis of the tendon.

In the principal reference frame (PAS) with the $\hat{z}_P$ axis oriented along the collagen fiber the diffusion tensor is given by

$$\overleftrightarrow{D}_{\mathrm{PAS}} = \begin{pmatrix} D_\perp & 0 & 0 \\ 0 & D_\perp & 0 \\ 0 & 0 & D_\parallel \end{pmatrix}, \tag{6}$$

where $D_\perp$ and $D_\parallel$ correspond to the self-diffusion coefficients oriented perpendicular and parallel to the $\hat{z}_P$ direction, respectively. In the laboratory reference frame (LF) with the $\hat{z}_L$ axis oriented along the magnetic field gradient the diffusion tensor can be written as

$$\overleftrightarrow{D}_{\mathrm{LF}} = R(\alpha,\beta,\gamma)\overleftrightarrow{D}_{\mathrm{PAS}}R^{-1}(\alpha,\beta,\gamma), \tag{7}$$

where $R(\alpha,\beta,\gamma)$ is the Euler rotation matrix defined for instance in [33]. The Euler angles (α,β,γ) describe the rotation from the PAS to the LF coordinate system.

For an uniaxial symmetric confinement of the free water in a tendon plug an average over the Euler angles α and γ (denoted by a bar) has to be performed. From Eqs. (6) and (7) we finally obtain for the angular average of the zz component of the diffusion tensor measured in LF:

$$\bar{D}_{zz}(\beta) = \sin^2\beta D_\perp + \cos^2\beta D_\parallel, \tag{8}$$

where $D_\parallel$ and $D_\perp$ correspond to the diffusion coefficient measured for the sample oriented at the angles $\beta = 0°$, and $\beta = 90°$, respectively. The polar angle β describes the orientation of the collagen fibril axis relative to the static magnetic field direction.

The constant relaxation method and the NMR-MOUSE were employed for measuring $D(\Theta)$ of free water in bovine Achilles tendon for three orientations $\Theta = 0°$, 35°, and 90° of the tendon plug axis relative to the symmetry axis of the sensor. The main contribution to the Hahn echo comes from the free water. The spin coherences from the protons of the collagen fibrils and bound water are not refocused at the position of the Hahn echo. The experimental values of diffusion coefficients obtained by fitting the experimental data according to the numerical procedure described in chapter 2 are shown in Fig. 11a. A monotonic change in the diffusivity versus the orientation angle Θ is observed as described by Eq. (8).

The orientation angle between the axes of the tendon and the permanent magnet axis is denoted by Θ. It is slightly different from the angle β. This is because the collagen fibers have a small angular distribution around the tendon symmetry axis that can be described by a Gaussian angular distribution function with a standard deviation of $\sigma \approx 13°$ and a center of distribution at

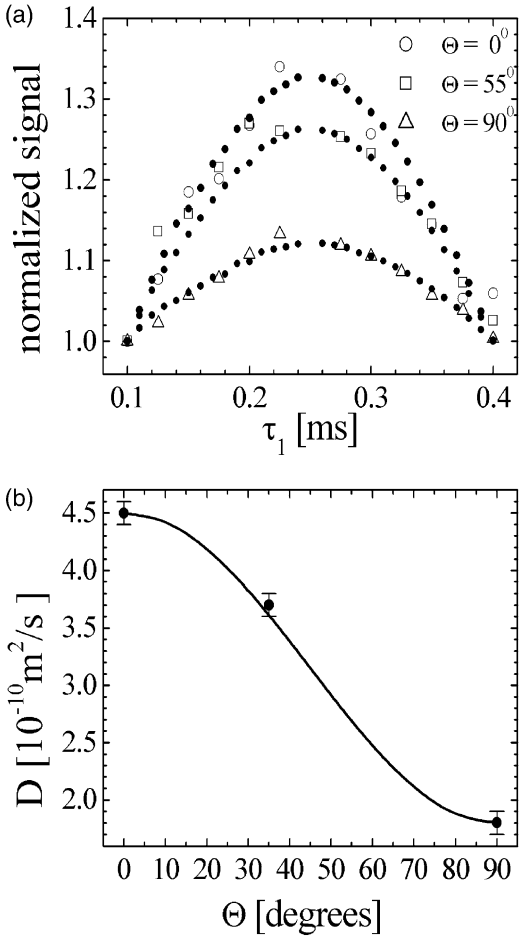

Fig. 11. (a) Measured (open symbols) and simulated (black circles) normalized Hahn-echo amplitudes for the constant time relaxation method with $\tau_1 + \tau_2 = 0.5$ ms on a plug of bovine Achilles tendon oriented at three angles Θ relative to the z-axis of the bar magnet. The values of the diffusion coefficients obtained from the simulation are shown versus angle Θ in (b). The angular dependence of the self-diffusion coefficients predicted by Eq. (8) with the measured values of $D_\perp$ and $D_\parallel$ is shown by the continuous line.

about 4° [34]. Moreover in the selective volume the directions of the field gradients are not strictly parallel to the axis of the cylindrical permanent magnet. Nevertheless, in the limit of these approximations it is expected that the diffusion coefficient $\bar{D}_{zz}(\beta)$ is not very different from $D(\Theta)$.

Because $D(\Theta = 0°) > D(\Theta = 90°)$ the volume explored by diffusion of the free water molecules is extended along the collagen fibrils. Using Eq. (8) one can predict the value of the diffusion coefficients at any orientation angle $\bar{D}_{zz}(\beta) \approx D(\Theta)$ from the coefficients $D(\Theta = 0°)$ and $D(\Theta = 90°)$ (see continuous line in Fig. 11b). For instance, one obtain the value $D(\Theta = 35°) = 3.6 \times 10^{-10}$ m^2/s, which is close to the measured value of $(3.7 \pm 0.1) \times 10^{-10}$ m^2/s. The anisotropy ratio $D(\Theta = 0°)/D(\Theta = 90°)$ can be evaluated from the data shown in Fig. 11b and has the value 2.5. The anisotropy of the tendon seems to be bigger by a factor of 1.5 than the values measured for both white matter and the optic nerve [32].

6. Conclusions

A new NMR-MOUSE with a bar permanent magnet was characterized in terms of the spatial distribution of the static and radiofrequency magnetic fields and the selective volume. Moreover, the distribution of field gradients of the first order was evaluated numerically in the selective volume.

A constant relaxation method using the Hahn spin echo generated by the pulse sequence $\theta_x - \tau_1 - 2\theta_y - \tau_1 + \tau_2 - 2\theta_y - \tau_2 - \textit{Hahn echo}$ with $\tau_1 + \tau_2 = \text{const.}$ was investigated for its use in strongly inhomogeneous static and radiofrequency magnetic fields of the bar-magnet NMR-MOUSE. A C++ program was written which is able to describe the strength of the Hahn-spin echo of a collection of isolated spins by taking into account the encoding of the coherences and z polarizations by molecular diffusion. This program has as input files the maps of B_0, B_1 and the filed gradient. Once the NMR sensor has been characterized by field mapping and the numerical procedure tested with a sample of a well-known diffusion coefficient the device can be used for the measurements of self-diffusion coefficient in a broad range of values. The high value of the average field gradient of the order of $G \approx 30$ T/m allows the measurements of self-diffusion coefficient as low as $D \approx 10^{-16}$ m^2/s. Even lower values can be measured if pulse sequences, which exploit both the static and radiofrequency field gradients, are used.

The bar-magnet NMR-MOUSE was used for measuring the diffusion coefficients of solvents swollen in crosslinked elastomers. The experiments were performed on a series of samples of natural rubber and showed that the diffusion coefficients can be correlated with the crosslink density and the shear modulus of the elastomers. This technique constitutes an alternative to measuring the transverse magnetization relaxation [7] for information about the crosslink density of elastomers.

The constant relaxation time method in strongly inhomogeneous magnetic fields can also be used to characterize the anisotropy of the diffusion coefficient of free water in biological tissues, which has been demonstrated for Achilles tendon. This shows that the mobile NMR sensor is able to assess the degree of order in connective tissues by the self-diffusion measurements.

Acknowledgments

This work was supported by a grant from Deutsche Forschungsgemeinschaft (DE 780/1-1). We are grateful to Dr. S. Anferova, Prof. Dr. V. Anferov, M. Adams,

and K. Kupferschläger for technical assistance. The authors are also grateful to Dr. K. Unseld and Dr. V. Hermann, Dunlop GmbH, Hanau, for providing the natural rubber samples and for helpful information.

References

[1] P.J. McDonald, Stray field magnetic resonance imaging, Prog. Nucl. Magn. Reson. Spect. 30 (1997) 69–99 (and references therein).
[2] R.L. Klinberg, A. Sezginer, D.D. Griffin, M. Fukuhara, Novel NMR apparatus for investigating an external sample, J. Magn. Reson. 97 (1992) 466–485.
[3] G. Eidmann, R. Savelsberg, P. Blümler, B. Blümich, The NMR MOUSE, a mobile universal surface explorer, J. Magn. Reson. A 122 (1992) 104–109.
[4] F. Balibanu, K. Hailu, K. Eymael, D.E. Demco, B. Blümich, Nuclear magnetic resonance in inhomogeneous magnetic fields, J. Magn. Reson. 145 (2000) 246–258.
[5] A. Wiesmath, C. Filip, D.E. Demco, B. Blümich, Double-quantum filtered NMR signals in inhomogeneous magnetic fields, J. Magn. Reson. 149 (2001) 258–263.
[6] A. Wiesmath, D.E. Demco, B. Blümich, NMR of multipolar spin states excited in strongly inhomogeneous magnetic fields, J. Magn. Reson. 154 (2002) 60–72.
[7] K. Hailu, R. Fechete, D.E. Demco, B. Blümich, Segmental anisotropy in strained elastomers detected with a portable NMR scanner, Solid State Nucl. Magn. Reson. 22 (2002) 327–343.
[8] R. Haken, B. Blümich, Anisotropy in tendon investigated in vivo by a portable NMR scanner, J. Magn. Reson. 144 (2000) 195–199.
[9] R.L. Klingberg, in: Encyclopedia of Nuclear Magnetic Resonance, vol. 8, Wiley, 1996, pp. 4960–4969, chapter Well logging.
[10] G. Goelman, M.G. Prammer, The CPMG pulse sequence in strong magnetic field gradients with applications to oil-well logging, J. Magn. Reson. A 113 (1995) 11–18.
[11] M.D. Hürlimann, D.D. Griffin, Spin dynamics of Carr–Purcell–Meiboom–Gill-like sequences in grossly inhomogeneous B_0 and B_1 fields and application to NMR well logging, J. Magn. Reson. 143 (2000) 120–135.
[12] M.D. Hürlimann, Diffusion and relaxation effects in general stray field NMR experiments, J. Magn. Reson. 148 (2001) 367–378.
[13] C.A. Meriles, D. Sakellariou, H. Heise, A.J. Moulé, A. Pines, Approach to high-resolution ex situ NMR spectroscopy, Science 293 (2001) 82–85.
[14] H. Heise, D. Sakellariou, C.A. Meriles, A.J. Moulé, A. Pines, Two-dimensional high-resolution NMR spectra in matched B_0 and B_1 field gradients, J. Magn. Reson. 156 (2001) 146–151.
[15] C. Meriles, D. Sakellariou, A. Pines, Resolved magic-angle spinning of anisotropic samples in inhomogeneous fields, Chem. Phys. Lett. 358 (2002) 391–395.
[16] R. Kimmich, W. Unrath, G. Schnur, E. Rommel, NMR measurements of small diffusion experiments in the fringe field of superconducting magnets, J. Magn. Reson. 91 (1991) 136–140.
[17] R. Kimmich, E. Fisher, One dimensional and two dimensional pulse sequences for diffusion experiments in the fringe field of superconducting magnets, J. Magn. Reson. A 106 (1994) 229–235.
[18] G. Fleischer, F. Fujara, Segmental diffusion in polymer melts and solutions of poly(ethylene oxide) measured with field gradient NMR in high-field gradients, Macromolecules 25 (1992) 4210–4219.
[19] D.E. Demco, A. Johansson, J. Tegenfeldt, Constant-relaxation methods for diffusion measurements in the fringe field of superconducting magnets, J. Magn. Reson. A 110 (1994) 183–193.
[20] A. Scharfenecker, I. Ardelean, R. Kimmich, Diffusion measurements with the aid of nutation spin echoes appearing after two inhomogeneous radiofrequency pulses in inhomogeneous magnetic fields, J. Magn. Reson. 148 (2001) 363–366.
[21] P.T. Callaghan, Principles of Magnetic Resonance Microscopy, Clarendon Press, Oxford, 1991.
[22] R. Kimmich, NMR: Tomography, Diffusiometry, Relaxometry, Springer-Verlag, Berlin, Heidelberg, New York, 1997.
[23] T.J. Norwood, R.A. Quilter, A robust NMR method for studying diffusion, J. Magn. Reson. 97 (1992) 99–110.
[24] D.E. Woessner, Effects of diffusion in nuclear magnetic resonance spin-echo experiments, J. Chem. Phys. 34 (1961) 2057–2061.
[25] R. Kaiser, E. Bartholdi, R.R. Ernst, Diffusion and field-gradient effects in NMR Fourier spectroscopy, J. Chem. Phys. 60 (1974) 2966–2979.
[26] B. Blümich (private communication).
[27] B. Blümich, V. Anferov, S. Anferova, M. Klein, R. Fechete, M. Adams, F. Casanova, Simple NMR-MOUSE with a bar magnet, Conc. Magn. Reson. (Magn. Reson. Eng.) 15 (2002) 255–261.
[28] E.D. van Meerwall, Self-diffusion in polymer systems measured with field-gradient spin echo NMR methods, Adv. Polym. Sci. 54 (1983) 1–29.
[29] E.D. van Meerwall, D. Shook, Self-diffusion of C_6F_6 in filled rubbery polymers, J. Appl. Phys. 56 (1984) 2444–2447.
[30] J.S. Ventras, C.M. Ventras, Solvent self-diffusion in rubbery polymer–solvent system, Macromolecules 27 (1994) 4684–4690.
[31] U. Sinha, L. Yao, In vivo diffusion tensor imaging of human calf muscle, J. Magn. Reson. Imag. 15 (2002) 87–95 (and references therein).
[32] R.M. Henkelman, G.J. Stanisz, J.K. Kim, M.J. Bronskill, Anisotropy of NMR properties of tissues, Magn. Reson. Med. 32 (1994) 592–601.
[33] K. Schmidt-Rohr, H.W. Spiess, Multidimensional Solid-state NMR and Polymers, Academic Press, London, 1994.
[34] R. Fechete, D.E. Demco, B. Blümich, U. Eliav, G. Navon, Anisotropy of collagen fiber orientation in sheep tendon by ^{1}H double-quantum-filtered NMR signals, J. Magn. Reson. 162 (2003) 166–175.